View metadata, citation and similar papers at core.ac.uk

brought to you by CORE

provided by Kyutacar : Kyushu Institute of Technology Academic Repository

Thermoelectric properties of n-type nanocrystalline bismuth-telluride-based thin films deposited by flash evaporation

著者	Takashiri M, Takiishi M, Tanaka S, Miyazaki Koji, Tsukamoto Hiroshi
journal or publication title	Journal of Applied Physics
volume	101
number	074301
page range	074301-1-074301-5
year	2007-04-04
URL	http://hdl.handle.net/10228/576

doi: 10.1063/1.2717867

Thermoelectric properties of *n*-type nanocrystalline bismuth-telluride-based thin films deposited by flash evaporation

M. Takashiri[a)]
Research Division, Komatsu Ltd., 1200 Manda, Hiratsuka, Kanagawa 254-8567, Japan

M. Takiishi, S. Tanaka, K. Miyazaki, and H. Tsukamoto
Department of Biological Functions and Engineering, Kyushu Institute of Technology, 2-4 Hibikino, Wakamatsu-ku, Kitakyushu Fukuoka 808-0196, Japan

(Received 3 October 2006; accepted 12 February 2007; published online 4 April 2007)

The thermal conductivity of *n*-type nanocrystalline bismuth-telluride-based thin films ($Bi_{2.0}Te_{2.7}Se_{0.3}$) is investigated by a differential 3ω method at room temperature. The nanocrystalline thin films are grown on a glass substrate by a flash evaporation method, followed by hydrogen annealing at 250 °C. The structure of the thin films is studied by means of atomic force microscopy, x-ray diffraction, and energy-dispersive x-ray spectroscopy. The thin films exhibit an average grain size of 60 nm and a cross-plane thermal conductivity of 0.8 W/m K. The in-plane electrical conductivity and in-plane Seebeck coefficient are also investigated. Assuming that the in-plane thermal conductivity of the thin films is identical to that of the cross-plane direction, the in-plane figure of merit of the thin films is estimated to be $ZT=0.7$. As compared with a sintered bulk sample with average grain size of 30 μm and nearly the same composition as the thin films, the nanocrystalline thin films show approximately a 50% reduction in the thermal conductivity, but the electrical conductivity also falls 40%. The reduced thermal and electrical conductivities are attributed to increased carrier trapping and scattering in the nanocrystalline film. © *2007 American Institute of Physics*. [DOI: 10.1063/1.2717867]

I. INTRODUCTION

Nanostructured materials have recently proven interesting in various fields because they have properties that differ attractively from those of bulk materials. For thermoelectric materials, the performance is enhanced in such nanosize structures as superlattices,[1–3] quantum dot superlattices,[4,5] and nanocomposites.[6,7] The performance of thermoelectric materials depends on the thermoelectric figure of merit, ZT, which is defined as $ZT=\sigma S^2 T/\kappa$, where σ is the electrical conductivity, S is the Seebeck coefficient, κ is the thermal conductivity, and T is the absolute temperature. The product σS^2 is defined as the thermoelectric power factor. The thermoelectric power factor should be maximized and the thermal conductivity should be minimized in order to achieve thermoelectric materials with high energy conversion efficiency.

Bismuth-telluride-based alloys are known to have excellent thermoelectric performance at room temperature because of their low thermal conductivity combined with high electrical conductivity and Seebeck coefficient compared to other thermoelectric materials. One approach to further reduce the thermal conductivity is to minimize the grain size of the materials. There are some reports of reduced thermal conductivity due to heat carrier scattering at grain boundaries.[8,9] Kim *et al.* reported reduced thermal conductivity in fine-grained Bi_2Te_3 sintered bulk alloys with grain sizes ranging from 1.2–3.9 μm.[10] Even though they fabricated Bi_2Te_3 powders with an average size of 150 nm, the grains grew significantly during the hot-pressing process. Therefore, it is challenging to prepare bulk materials with nanosize grains.

Thin-film technology may be advantageous for fabricating bismuth-telluride-based materials with fine grain sizes. In particular, the flash evaporation method is ideal because the thin films are deposited so rapidly on a substrate that there is little time for the grains to grow larger. After the initial deposition of fine-grained thin films, the grain size can be increased controllably to the desired size by an annealing process. The annealing process also helps enhance the thermoelectric properties of the thin film by reducing defects and improving the crystallinity. Many researchers have obtained bismuth-telluride-based thin films with high performance.[11–14] However, previous studies of the thin films were not focused on nanosize grains and their thermal properties.

The 3ω method is one reliable technique for measuring the thermal conductivity of thin films.[15–17] The 3ω method requires preparation of a dielectric thin film and a metallic thin wire on a thermoelectric thin film. Generally, the thin metallic wire is fabricated by using lithography and other semiconductor processes. However, these facilities are expensive, and there are restrictions about sharing processing equipment with silicon-based materials due to concerns about contaminating the silicon materials with heavy metals.

In this study, we measure the thermal conductivity of *n*-type nanocrystalline bismuth-telluride-based thin films by a differential 3ω method at room temperature. The metallic heater wire is fabricated by an electron beam deposition method using fine-line shadow masks. The electrical conductivity, Seebeck coefficient, and thermoelectric power factor

[a)]Author to whom correspondence should be addressed; electronic mail: masayuki_takashiri@komatsu.co.jp

 © 2007 American Institute of Physics

Downloaded 26 Dec 2007 to 150.69.123.200. Redistribution subject to AIP license or copyright; see http://jap.aip.org/jap/copyright.jsp

are also investigated. The nanocrystalline thin films are prepared by a flash evaporation method and then annealed at a temperature of 250 °C in a hydrogen atmosphere. The average grain size of the thin films is estimated using an atomic force microscope (AFM). The transport properties of the nanocrystalline thin films are compared with a sintered bulk sample with microsize grains.

II. EXPERIMENT

The n-type nanocrystalline bismuth-telluride-based thin films are fabricated on glass substrates (Corning 7059) by a flash evaporation method. The flash evaporation equipment is described elsewhere.[18] The starting material for the flash evaporation is n-type $Bi_{2.0}Te_{2.7}Se_{0.3}$ spherical powders with average powder size of 200 μm by a centrifugal atomization method. Inside the flash evaporation chamber the distance between the tungsten boat and the substrate is 200 mm. When the chamber is evacuated to 1.4×10^{-3} Pa, we apply a current of 80 A to the tungsten boat until the substrate temperature reaches 200 °C. The thickness of the deposited thin films is 0.75 μm.

A hydrogen annealing process is used to enhance the thermoelectric properties of the nanocrystalline thin films.[19] Samples are placed in an electric furnace that is evacuated to 1.0 Pa and purged five times with high-purity (99.999%) argon gas. Then, the furnace is filled with hydrogen gas at atmospheric pressure, and the hydrogen gas flow rate is maintained at 0.3 slm throughout the annealing process. The temperature is increased steadily at 5 K/min to 250 °C, and the samples are then annealed at 250 °C for 30 min. After annealing, the samples are cooled down naturally to room temperature.

The surface morphology, crystallization, and composition of the nanocrystalline thin films are investigated by means of atomic force microscopy (AFM), x-ray diffraction (XRD), and energy-dispersive x-ray analysis (EDX). The in-plane electrical conductivity σ of the nanocrystalline thin films is measured at room temperature by a four-point probe method with accuracy of ±3%. The in-plane Seebeck coefficient S is also measured at room temperature with accuracy of ±5%. One end of the thin film is connected to a heat sink and the other end to a heater. The Seebeck coefficient is determined as the ratio of the potential difference (ΔV) along the films to the temperature difference (ΔT). The thermoelectric power factor σS^2 is estimated from the results of the electrical conductivity and the Seebeck coefficient.

The cross-plane thermal conductivity is determined at room temperature by a differential 3ω method with accuracy of ±10%.[8] Details of the thermal conductivity measurement are described in previous publications.[20,21] In brief, the 3ω method for thin films uses a single metal thin wire as both the heater and thermometer (see the inset of Fig. 6). An ac driving current at angular frequency ω heats the surface of the dielectric films at a frequency 2ω. Since the resistance of a pure metal increases with temperature, these temperature fluctuations also cause fluctuations of the electrical resistance at a frequency of 2ω. Consequently, the voltage drop across the metal wire has a small component at 3ω that can be used to measure the temperature fluctuations and therefore the thermal response of the dielectric films and substrate.

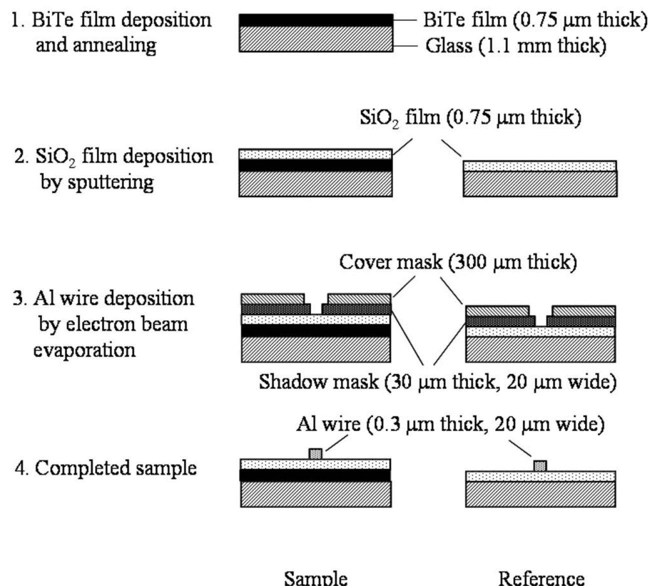

FIG. 1. Schematic flow chart of the fabrication process of samples for the measurement of the thermal conductivity using the 3ω method.

Figure 1 shows the schematic flow chart of the fabrication process of samples for the measurement of the thermal conductivity using the 3ω method. Our process consists of three main steps. First, a 0.75 μm thick bismuth-telluride-based thin film is deposited and annealed. Second, a 0.75 μm thick SiO_2 thin film is deposited on the bismuth-telluride-based thin film by a sputtering method. Third, the thin aluminum heater wire is deposited on the sample by electron beam evaporation through a shadow mask. The aluminum is patterned using a double shadow mask structure. A 30 μm thick shadow mask with 20 μm width line pattern is placed on the sample; then, a 300 μm thick shadow mask with 500 μm width line pattern is aligned on top of the 30 μm thick shadow mask. This is because the 30 μm thick shadow mask can be easily bent during the aluminum deposition, causing the thin line to blur and widen, so we use the 300 μm thick shadow mask to strengthen the 30 μm thick shadow mask and prevent it from bending. We also fabricate reference samples that lack the bismuth-telluride-based thin film but are otherwise identical to the primary samples. The reference samples are used to subtract off the unknown thermal properties of the insulation layers. Figure 2 shows photographs of the completed sample and reference for the measurement of thermal conductivity. The dimensions of the thin aluminum wire are exactly the same for both the sample and the reference. The thin aluminum wire is 20 μm wide and the heater length is 2 mm. The sample with bismuth-telluride-based thin films is 25 mm long, 5 mm wide, and 1.1 mm thick, and the reference sample is 50 mm long, 25 mm wide, and 1.1 mm thick. Because the bismuth-telluride thin film (0.75 μm thick) and the SiO_2 film (0.75 μm thick) are far thinner than the width of the heater, the direction of heat flow can be considered as perpendicular to the thin film.

Downloaded 26 Dec 2007 to 150.69.123.200. Redistribution subject to AIP license or copyright; see http://jap.aip.org/jap/copyright.jsp

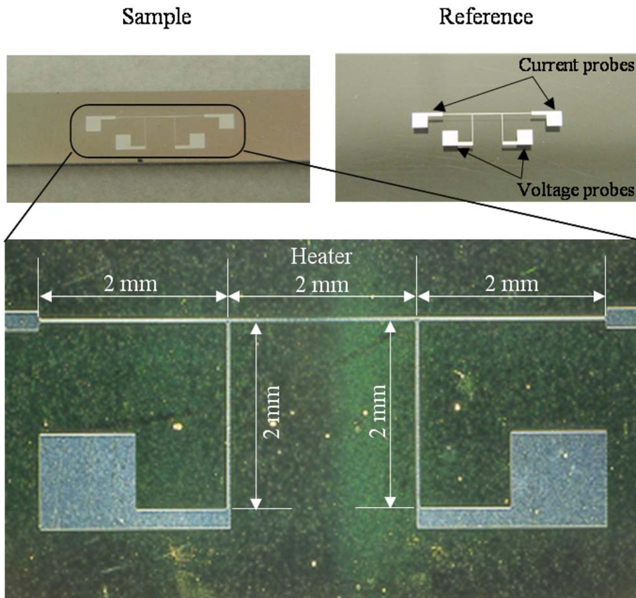

FIG. 2. (Color online) Images of the samples used for the measurement of thermal conductivity using the 3ω method.

III. RESULTS AND DISCUSSION

The surface morphology and the grain structure of the *n*-type nanocrystalline bismuth-telluride-based thin films are characterized by AFM (Fig. 3). To make the grain structure clear, the grain boundaries are drawn by solid lines on the right half of the image. The thin films are continuous with no porosity, exhibit grain sizes around 100 nm, and have surface flatness less than 10 nm. The distribution of grain sizes of the thin films is estimated from the AFM image by an imaging processing software to trace out the grain boundaries. Figure 4 shows the distribution of grain sizes, revealing that the thin films are composed of grains ranging in size from 10 to 160 nm, with the average grain size being approximately 60 nm.

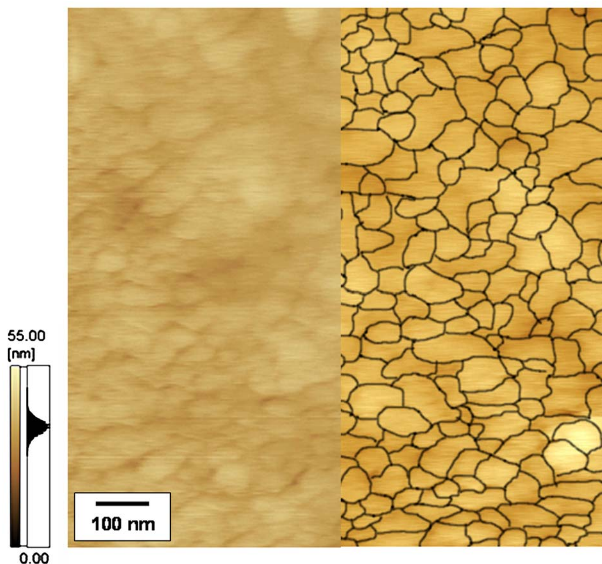

FIG. 3. (Color online) Surface morphology and grain structure of the *n*-type nanocrystalline bismuth-telluride-based thin films studied by AFM. To make the grain structure clear, the grain boundaries are drawn by solid lines on the right half of the image.

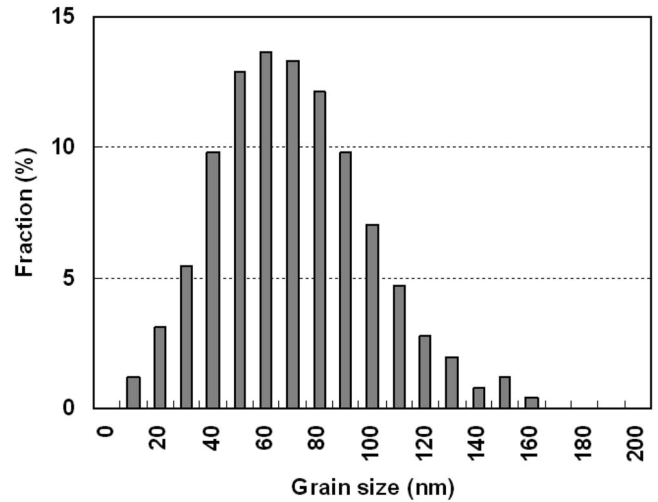

FIG. 4. Grain size distribution of *n*-type bismuth-telluride-based thin films. Fraction of total number in population of grains against grain diameter (size).

The crystallization and orientation of the nanocrystalline thin films are investigated by XRD (Fig. 5). The XRD pattern of the nanocrystalline thin films is found to exhibit multiple peaks. The intensity ratio of the sum of all of the *c*-axis oriented peaks, $\Sigma\{001\}$, to the sum of all of the peaks, $\Sigma\{hkl\}$, is estimated as 0.41. This result indicates that the nanocrystalline thin films do not have any preferred crystal orientation. We also estimate the average grain size of the thin films from the full-width at half maximum of the XRD peaks using Scherrer's equation. The average grain size is thus estimated as 58 nm, which is consistent with the estimate from the AFM analysis in Fig. 4.

EDX provides the atomic composition of the initial *n*-type bismuth-telluride-based powders and of the resulting nanocrystalline thin films (Table I). The composition of the powders is stoichiometric. The composition of the nanocrystalline thin films deviates slightly from stoichiometry, revealing a slightly tellurium-rich structure.

Figure 6 shows experimentally measured temperature

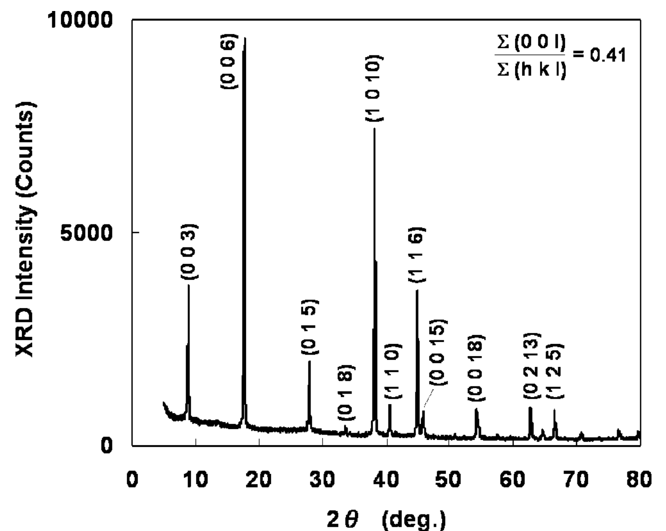

FIG. 5. X-ray diffraction pattern of the *n*-type nanocrystalline bismuth-telluride-based thin film.

Downloaded 26 Dec 2007 to 150.69.123.200. Redistribution subject to AIP license or copyright; see http://jap.aip.org/jap/copyright.jsp

TABLE I. The atomic composition of the starting powders and resulting thin films, as determined by EDX.

Samples	Bi (at. %)	Te (at. %)	Se (at. %)
Powders	40	54	6
Nanocrystalline thin films by flash evaporation	38	57	5

amplitudes experienced by a 20 μm wide heater on both the reference sample and the sample with the bismuth-telluride-based thin film. The thermal conductivity of the nanocrystalline thin films is extracted from a curve fit of the measured temperature difference.[16,17] As a result, the cross-plane thermal conductivity of the nanocrystalline thin films is determined to be 0.8 W/m K at room temperature. We assume that the in-plane thermal conductivity of the thin films is similar to the cross-plane thermal conductivity because the XRD patterns indicate that the thin films do not have any preferred crystal orientation.

In order to compare the thermoelectric properties of the nanocrystalline thin films with those of bulk materials with larger grains, we also fabricate a sintered bulk sample by a hot-pressing method and measure the thermal conductivity by laser flash method. We expect the Seebeck coefficient of the sintered bulk sample to be similar to the nanocrystalline thin films. The average grain size of the sintered bulk sample is approximately 30 μm. The composition of the sintered bulk sample is the same as the powders for the fabrication of the thin films, and we confirm that the bulk sample does not exhibit any preferred crystal orientation.

The transport properties of the nanocrystalline thin films and the sintered bulk sample are shown in Table II. The thermal conductivity of the nanocrystalline thin films is reduced to 0.8 W/m K in the cross-plane direction. The electrical conductivity and the Seebeck coefficient of the thin films are 0.54×10^5 (S/m) and -186.1 μV/K in the in-plane direction, respectively. Assuming that the in-plane thermal conductivity of the nanocrystalline thin films is identical to that of the cross-plane direction, the figure of merit of the thin films is estimated to be $ZT=0.7$. The figure of merit of the nanocrystalline thin films is only 0.1 larger than that of the sintered bulk sample, even though the thermal conductivity of the nanocrystalline thin films is approximately 50% smaller than the sintered bulk sample. This is because the electrical conductivity of the nanocrystalline thin films is also reduced. We believe that enhanced heat carrier scattering due to the nanocrystalline structure of the thin films and carrier trapping at grain boundaries are responsible for the measured reductions in both the thermal and electrical conductivities.

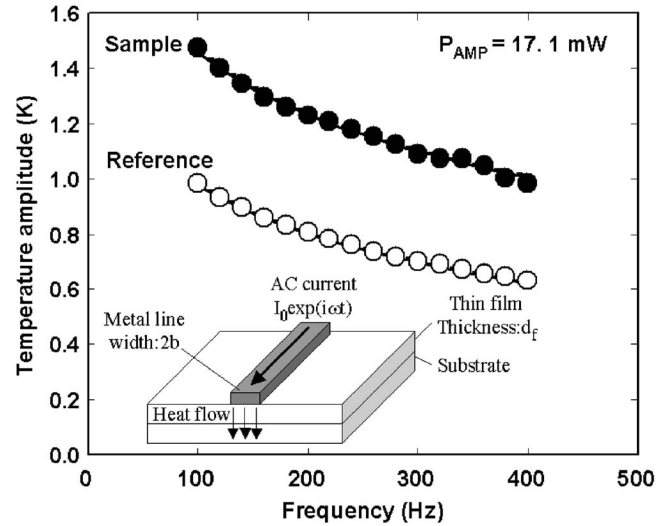

FIG. 6. The temperature amplitudes experienced by 20 μm width heaters deposited onto the reference and the *n*-type nanocrystalline bismuth-telluride-based thin-film sample.

To explore the changes in ZT more thoroughly, we estimate the lattice thermal conductivity (κ_l) and the electronic thermal conductivity (κ_e). The electronic thermal conductivity is calculated from the measured electrical conductivity by using the Wiedemann-Franz law, where the Lorenz number is taken to be $L=2.45\times10^{-8}$ WΩ/K^2. The lattice thermal conductivity is estimated by subtracting the calculated electronic thermal conductivity from the measured total thermal conductivity. The various thermal conductivities of the nanocrystalline thin films and the sintered bulk sample are shown in Table III. The lattice and electronic thermal conductivities of the nanocrystalline thin films are both 0.4 W/m K, while the sintered bulk sample has a lattice thermal conductivity of 0.9 W/m K and an electronic thermal conductivity of 0.7 W/m K. The ratio of the lattice thermal conductivity to the total thermal conductivity ($\kappa_l\kappa_{\rm total}$) is similar in both the nanocrystalline thin films and the sintered bulk sample. Therefore, we may conclude that both phonons and electrons are scattered or trapped at the grain boundaries in the nanocrystalline thin films. The reasons that the lattice thermal conductivity of the nanocrystalline thin films is not significantly reduced compared to the electronic thermal conductivity are not clear yet, but we expect that quantum size effects can be ignored because of the broad distribution of grain sizes and because the grains are still large compared to the electron and phonon wavelengths.

TABLE II. The transport properties of the *n*-type nanocrystalline bismuth-telluride-based thin films and the sintered bulk sample with average grain size of 30 μm.

Samples	Avg. grain size	κ (W/m K)	σ (S/m)	S (μV/K)	σS^2 (μW/cm K^2)	ZT (300 K)
Nanocrystalline thin film by flash evaporation	60 nm	0.8 (cross-plain)	0.54×10^5 (in-plane)	−186.1 (in-plane)	18.7 (in-plane)	0.7
Sintered bulk material by hot-pressing	30 μm	1.6	0.93×10^5	−177.5	29.3	0.6

Downloaded 26 Dec 2007 to 150.69.123.200. Redistribution subject to AIP license or copyright; see http://jap.aip.org/jap/copyright.jsp

TABLE III. The thermal conductivities of the *n*-type nanocrystalline bismuth-telluride-based thin films and the sintered bulk sample with average grain size of 30 μm.

Samples	κ_{total} (W/m K)	κ_l (W/m K)	κ_e (W/m K)	κ_l/κ_{total}
Nanocrystalline thin film by flash evaporation	0.8	0.4	0.4	0.50
Sintered bulk material by hot-processing	1.6	0.9	0.7	0.56

IV. CONCLUSION

In order to investigate the thermal conductivity of the *n*-type nanocrystalline bismuth-telluride-based materials, we deposited thin films on a glass substrate by a flash evaporation method, followed by a hydrogen annealing process at 250 °C. The thin films are tellurium rich and have grains with average size of 60 nm and no preferred crystal orientation. The cross-plane thermal conductivity of the nanocrystalline thin films is measured by a differential 3ω method at room temperature. The in-plane electrical conductivity and Seebeck coefficient are also investigated. The cross-plane thermal conductivity of the nanocrystalline thin films is 0.8 W/m K, about half of the value for a sintered bulk sample with average grain size of 30 μm and nearly the same composition as the nanocrystalline thin films. Assuming that the in-plane thermal conductivity of the nanocrystalline thin films is identical to that of the cross-plane direction, the figure of merit of the nanocrystalline thin films is estimated to be $ZT=0.7$. Compared to the sintered bulk sample, the nanocrystalline thin films exhibit an improvement of 0.1 in the *ZT* value. However, the percentage increase of the *ZT* value of the nanocrystalline thin films is smaller than the percentage decrease of its thermal conductivity. This is because the electrical conductivity of the nanocrystalline thin films is also reduced. Enhanced heat carrier scattering due to the nanocrystalline structure of the thin films and carrier trapping at grain boundaries are believed to be responsible for the measured reductions in the thermal and electrical conductivities. For a more detailed analysis, we also estimate the lattice and electronic contributions to the thermal conductivity, revealing that the ratio of the lattice thermal conductivity to the total thermal conductivity is similar in both the nanocrystalline thin film and the sintered bulk sample. Therefore, we may conclude that both phonons and electrons are scattered or trapped at the grain boundaries in the nanocrystalline thin films.

ACKNOWLEDGMENTS

This work is supported in part by the research program on development of innovative technology, the Japan Science and Technology Agency (JST). The authors wish to thank Professor Chen and Dr. Dames at the Massachusetts Institute of Technology for valuable comments, Dr. Jacquot at Fraunhofer Institut Physikalische Messtechnik in Germany for experimental support, thermoelectrics researchers at Komatsu Ltd. for their continuous encouragement, and the staff of the Analysis and Measurement Group at Komatsu Ltd. for technical support.

[1] M. Laroche, R. Carminati, and J.-J. Greffet, J. Appl. Phys. **100**, 063704 (2006).
[2] G. Zeng, J. E. Bowers, J. M. O. Zide, A. C. Gossard, W. Kim, S. Singer, A. Majumdar, R. Singh, Z. Bian, Y. Zhang, and A. Shakouri, Appl. Phys. Lett. **88**, 113502 (2006).
[3] T. Borca-Tasciuc, D. W. Song, J. R. Meyer, I. Vurgaftman, M.-J. Yang, B. Z. Nosho, L. J. Whitman, H. Lee, R. U. Martinelli, G. W. Turner, M. J. Manfra, and G. Chen, J. Appl. Phys. **92**, 4994 (2002).
[4] T. C. Harman, P. J. Taylor, M. P. Walsh, and B. E. LaForge, Science **297**, 2229 (2002).
[5] Y. Bao, A. A. Balandin, J. L. Liu, J. Liu, and Y. H. Xie, Appl. Phys. Lett. **84**, 3355 (2004).
[6] R. Yang and G. Chen, Phys. Rev. B **69**, 195316 (2004).
[7] X. B. Zhao, X. H. Ji, Y. H. Zhang, T. J. Zhu, J. P. Tu, and X. B. Zhang, Appl. Phys. Lett. **86**, 062111 (2005).
[8] M. Takashiri, T. Borca-Tasciuc, A. Jacquot, K. Miyazaki, and G. Chen, J. Appl. Phys. **100**, 054315 (2006).
[9] D. M. Rowe and V. S. Shukla, J. Appl. Phys. **52**, 7421 (1981).
[10] D.-H. Kim and T. Mitani, J. Alloy. Compd. **399**, 14 (2005).
[11] I.-H. Kim, Mater. Lett. **44**, 75 (2000).
[12] V. D. Das and R. C. Mallik, Solid State Commun. **120**, 217 (2001).
[13] A. Foucaran, A. Sackda, A. Giani, F. Pascal-Delannoy, and A. Boyer, Mater. Sci. Eng. B **52**, 154 (1998).
[14] F. Völklein, V. Baier, U. Dillner, and E. Kessler, Thin Solid Films **187**, 253 (1990).
[15] D. G. Cahill, Rev. Sci. Instrum. **61**, 802 (1990).
[16] D. G. Cahill, M. Katiyar, and J. R. Abelson, Phys. Rev. B **50**, 6077 (1994).
[17] S.-M. Lee and D. G. Cahill, J. Appl. Phys. **81**, 2590 (1997).
[18] M. Takashiri, T. Shirakawa, K. Miyazaki, and H. Tsukamoto, J. Alloys Compd. (in press).
[19] M. Takashiri, T. Shirakawa, K. Miyazaki, and H. Tsukamoto, Trans. Jpn. Soc. Mech. Eng., Ser. A **72**, 1793 (2006) (in Japanese).
[20] T. Borca-Tasciuc, A. R. Kumar, and G. Chen, Rev. Sci. Instrum. **72**, 2139 (2001).
[21] A. Jacquot, B. Lenoir, A. Dauscher, M. Stölzer, and J. Meusel, J. Appl. Phys. **91**, 4733 (2002).

Downloaded 26 Dec 2007 to 150.69.123.200. Redistribution subject to AIP license or copyright; see http://jap.aip.org/jap/copyright.jsp